

$E2$ and $E4$ Transition Moments and Equilibrium Deformations in the Actinide Nuclei*

C. E. Bemis, Jr., F. K. McGowan, J. L. C. Ford, Jr., W. T. Milner, P. H. Stelson, and R. L. Robinson
Oak Ridge National Laboratory, Oak Ridge, Tennessee 37830

(Received 30 May 1973)

Precision Coulomb-excitation experiments using ^4He ions have been performed in the actinide region ($230 \leq A \leq 248$) by the observation of elastic and inelastically scattered projectiles using a split-pole magnetic spectrometer equipped with a position-sensitive proportional detector. 12 even- A targets from ^{230}Th to ^{248}Cm have been investigated and the reduced quadrupole matrix element, $\langle 2 || \mathfrak{M}(E2) || 0 \rangle$, and the reduced hexadecapole matrix element, $\langle 4 || \mathfrak{M}(E4) || 0 \rangle$, have been determined from the experimental excitation probabilities of the 0^+ , 2^+ , and 4^+ states in the ground-state rotational bands. The values of $B(E4, 0 \rightarrow 4)$ range from 167 single-particle units for ^{234}U to essentially zero single-particle units for $^{244, 246, 248}\text{Cm}$. Model-dependent deformation parameters, β_{20} and β_{40} , are extracted from the measured $E2$ and $E4$ transition moments for distributions of nuclear charge represented by deformed Fermi distributions and by a deformed homogeneous distribution.

NUCLEAR REACTIONS $^{230, 232}\text{Th} (\alpha, \alpha')$, $^{236}\text{U} (\alpha, \alpha')$, $E=16$ and 17 MeV, $^{234}\text{U} (\alpha, \alpha')$, $E=16-19$ MeV, $^{238}\text{U} (\alpha, \alpha')$, $E=16-18$ MeV, $^{238, 240, 242, 244}\text{Pu} (\alpha, \alpha')$, $^{244, 246, 248}\text{Cm} (\alpha, \alpha')$, $E=17$ MeV; measured $\sigma(E_{\alpha'})$; $\theta=150^\circ$; deduced $B(E2)$, $B(E4)$. Enriched targets. Extracted model-dependent deformations, β_{20} and β_{40} .

I. INTRODUCTION

Theoretical predictions of deformation parameters for the ground state of actinide nuclei are based on calculations which minimize the total potential energy with respect to deformations. A comparison between theory and experiment for the equilibrium deformations and related quantities such as intrinsic multipole moments and transition moments is particularly valuable for these heavy nuclei since Nilsson *et al.*¹ have extended their calculations into the region of "superheavy" nuclei. The quality of agreement between theory and experiments in the actinide region is valuable in the difficult matter of assessing the level of confidence given to predictions of near stable "superheavy" elements.

Nilsson *et al.*¹ have used the deformed harmonic-oscillator potential, while Gareev, Ivanova, and Pashkevitch² and Alder *et al.*³ have used the Woods-Saxon potential for the single-particle structure. All calculations have used the "Strutinsky procedure"⁴ to normalize the shell structure to that of the liquid drop in order to obtain the potential-energy surface. One of the surprising results of these calculations are the relatively large P_4 (hexadecapole) deformations in addition to the usual P_2 (quadrupole) deformations which characterize the nuclei in both the rare-earth and actinide deformed regions. Inclusion of the P_4 term in the multipole expansion of the shape has an important effect on the calculated nuclear-structure properties for these nuclei such as ground-state masses, relative heights of fission

barriers and hence the fission properties, and on the ordering and relative spacing of levels, and wave functions of the single particle moving in the deformed potential. The single-particle effects primarily arise from the coupling between the oscillator shells with N and $N \pm 2$ which can be included explicitly by the inclusion of the P_4 term.

The inclusion of the P_4 term in the equilibrium shapes of deformed rare-earth nuclei has been well established in (α, α') experiments above the Coulomb barrier by Hendrie *et al.*⁵ and by Aponick *et al.*⁶ Pure electromagnetic probes of the nuclear charge distribution have been used subsequently to extract information about the higher-order deformation. Stephens *et al.*⁷ first demonstrated that Coulomb excitation with ^4He ions was a very useful technique for observing the $E4$ transitions in deformed even- A nuclei in their studies of ^{152}Sm and ^{154}Sm . These measurements have been extended throughout the entire rare-earth deformed region by Saladin and co-workers⁸ and by Shaw, Greenberg, and Hadsell.⁹ Inelastic electron scattering, another pure electromagnetic probe, has recently been used to determine moments higher than quadrupole in the ground-state charge distribution of ^{152}Sm .¹⁰ In recent experiments by Brückner *et al.*¹¹ the ^4He excitation of ^{152}Sm has been investigated both via Coulomb excitation and direct nuclear reactions. The equivalency of the nuclear charge-deformation parameters for ^{152}Sm , as measured by Coulomb excitation^{8, 11} and by inelastic electron scattering,¹⁰ with the potential or matter deformations, inferred from strong interaction probes such as

the (α , α') reaction at bombarding energies near and above the Coulomb barrier,^{5,11} seems to suggest that no significant differences exist between the two types of experiments. This equivalency is less clear however if the Coulomb excitation results of Refs. 7 and 9 are used as a basis for comparison. Both quadrupole and hexadecapole deformations for the rare-earth nuclei, therefore, are well established and the charge deformation appears nearly identical to the potential or matter deformation.

That the hexadecapole deformation be included in the multipole expansion of the nuclear shape in the actinide region has been suggested by α -decay experiments as early as 1957 by Fröman.¹² More recent treatments of α decay¹³ have included or considered the effect of the P_4 deformation. Inelastic proton-scattering experiments at 23 MeV have also been analyzed in terms of the higher-order moments by Moss *et al.*¹⁴ for ²³²Th and ²³⁸U. This work also suggests the importance of hexadecapole deformations in this mass region.

We have performed precision Coulomb-excitation experiments for even- A nuclei throughout the range of the actinide deformed region. Some of our preliminary results have already been published¹⁵ and have demonstrated that substantial equilibrium hexadecapole deformations, in addition to the quadrupole deformations, do exist in this region as manifested in the greatly enhanced $E4$ transitions observed in our experiments. Since the Coulomb excitation reaction is a pure electromagnetic probe and sensitive only to the electric multipole moments of the nucleus, valuable information about the charge deformation of the nuclear ground states may be derived from these experiments.¹⁶ This communication summarizes all of our Coulomb-excitation experiments for the ground-state rotational bands in the even- A actinide deformed region with ⁴He ions. Our experimental transition moments are used to extract charge-deformation parameters which are compared with theoretical predictions and with other experiments.

During the course of this work, an (α , α') scattering experiment at 50 MeV was completed for ²³⁸U.¹⁷ This work substantiates the large hexadecapole moments in this mass region as observed in our experiments.

II. EXPERIMENTAL METHOD

The experiments were performed using ⁴He ions accelerated in the EN tandem Van de Graaff at Oak Ridge National Laboratory. The ⁴He⁺⁺ ion beam was energy-analyzed using a 90° sector magnet system, deflected through an additional 90° sector magnet and focused to yield a narrow

line, ~ 1 mm wide \times 3 mm high, at the target position of a split-pole magnetic spectrometer. Elastically and inelastically scattered ions from the targets were observed at a laboratory angle of 150° using the spectrometer which was equipped with a 20-cm-long position-sensitive gas proportional detector in the focal plane. This detector, developed by Borkowski and Kopp,¹⁸ consists of a single high-resistivity central anode with position information derived from the difference in rise times of the pulses at the ends of the detector. The pulses at both ends of the counter were also summed and the energy sum pulse, ~ 1 MeV for 17-MeV α particles, was used to discriminate against multiple scattering and other background effects not originating in the actinide targets or target backings. A complete description of this detector and performance data for ⁴He ions in the Enge spectrometer have been reported in detail by Ford, Stelson, and Robinson.¹⁹ Under the conditions of our experiment, it was possible to obtain an energy resolution of 15 keV full width at half maximum for scattered ⁴He ions which is more than adequate to separate the ground band rotational states in the even- A actinide nuclei.

Isotopically pure targets of the even- A actinides that were studied in this work include ^{230, 232}Th, ^{234, 236, 238}U, ^{238, 240, 242, 244}Pu, and ^{244, 246, 248}Cm. The targets were prepared using a 150-cm radius 90° sector electromagnetic isotope separator.²⁰ Ions were produced using ~ 50 μ g of the oxide as charge material by the CCl₄ technique²⁰ and an oscillating-electron-type discharge source. The separations were performed at 80-kV accelerating potential but collections were made at an incident ion energy of ~ 3 keV using a strong focusing electrostatic retardation lens. This retardation lens was adjusted to yield a rectangular target spot, 1 mm \times 6 mm, which is a nearly ideal source width for the Enge split-pole spectrograph. Target backings for most of the experiments were 1.27×10^{-4} -cm-thick Ni although in later experiments, 40- μ g/cm² carbon foils were used to avoid heavy-element impurities that were present in the Ni foils. In all cases, ~ 1 μ g of the target material was collected in the separator which yielded target thicknesses of 20–30 μ g/cm² implanted at a depth of ~ 1 μ g/cm² in the target backing. Since all experiments were performed in backscattering geometry, the relatively thick Ni target backings posed no problem in energy resolution yet allowed a measure of protection against breakage of the highly α -radioactive targets.

Calibration of the Enge spectrometer and position-sensitive counter system was accomplished using a ²⁴⁴Cm α source placed in the normal target position of the spectrometer scattering cham-

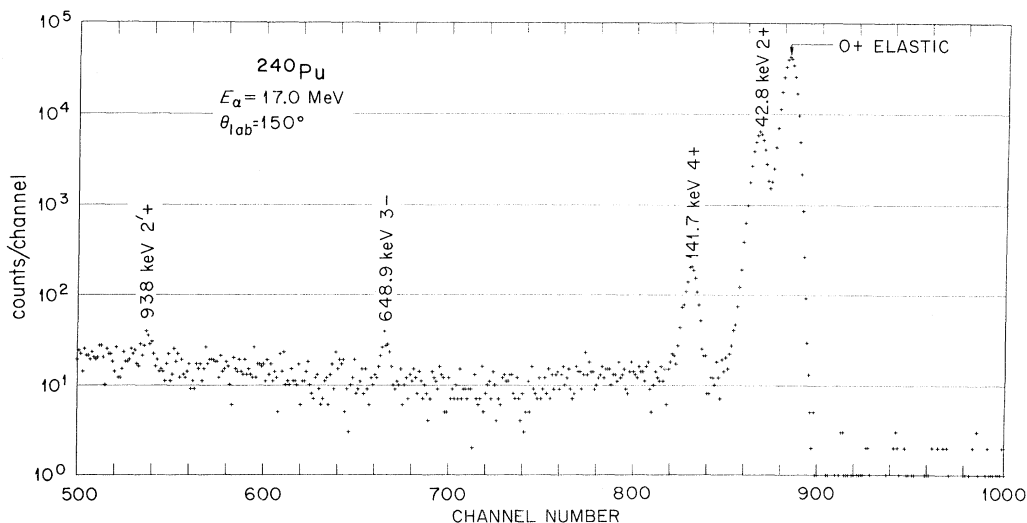


FIG. 1. Elastically and inelastically scattered 17-MeV ^4He ions from ^{240}Pu at a laboratory angle of 150° . The background below the ^{240}Pu 4^+ peak arises from ~ 40 ppm of Pb and other heavy-element impurities uniformly distributed in the Ni target backing.

ber. The 5804.958 ± 0.050 - and 5762.835 ± 0.030 -keV α groups²¹ provided convenient spectrometer field calibration points together with position linearity and efficiency checks for the counter as these groups were moved along the length of the counter in given spectrometer magnetic-field increments. The position information from the detector was digitized and stored using a 1024-channel pulse-height analyzer.

III. RESULTS

Typical scattered ^4He ion spectra as observed in our experiments are shown in Figs. 1 and 2 for

^{240}Pu and ^{232}Th , respectively. The ^{240}Pu spectrum in Fig. 1 shows the effect of a small Pb impurity in the thick Ni target backing and the ^{232}Th spectrum in Fig. 2 shows the thin-target effect of about 0.5 ng of ^{181}Ta impurity which arose during target preparation in the isotope separator. In all cases, target impurities did not effect the extraction of the excitation probabilities for the 2^+ and 4^+ states relative to the elastic scattering peak. These subtle effects, however, clearly emphasize the need for isotopically pure targets as produced in an isotope separator.

Other states at higher excitation energies than

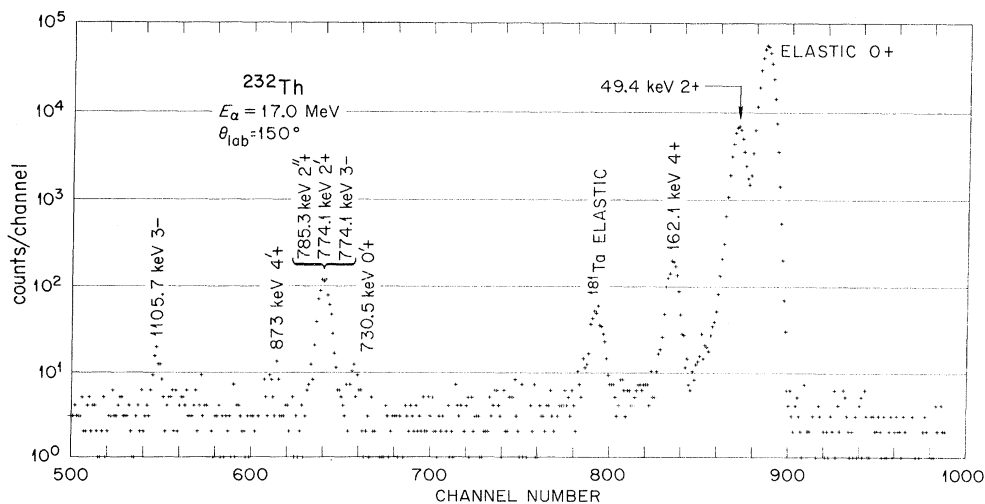


FIG. 2. Elastically and inelastically scattered 17-MeV ^4He ions from ^{232}Th at a laboratory angle of 150° using a carbon foil as the target backing. Peak-to-background ratio is approximately 20 000 to 1. The ^{181}Ta contamination from the $\text{Ta}^{16}\text{O}^{35}\text{Cl}^+$ molecular ion which was collected at the ^{232}Th position in the isotope separator.

the 2^+ and 4^+ states in the ground-state rotational band were also measured in our experiments as can be seen in Figs. 1 and 2. These states are primarily excited by direct $E2$ and $E3$ Coulomb-excitation processes and in most cases, where detailed information from nuclear spectroscopic studies are available, could be identified with known states. The β -vibrational-like $2'^+$ and $4'^+$ states, the γ -vibrational-like $2''^+$ state, and a 3⁻ member of the intrinsic octupole quadruplet ($K=0^-, 1^-, 2^-, 3^-$) are among the higher states that were excited and will be the subject of a future publication.²² However, the influence of these states on the excitation probabilities of states in the ground-state rotational band have been considered in the analyses.

The experimental excitation probabilities for the 2^+ and 4^+ ground band rotational states were determined relative to the elastic scattering peak by means of a peak-shape analysis which required the 2^+ and 4^+ peaks to have the same shape as the elastic scattering peak. Iterative fits to the spectrum were performed both by hand-fitting procedures and using a computer routine²³ to simultaneously fit all three peaks and the background until the experimental spectrum was reproduced. In general the excitation probabilities were determined relative to the elastic peak from the measured peak areas with an accuracy of $\sim 1\%$ for the 2^+ states and 3 to 4% for the 4^+ states. These errors include uncertainties in background subtraction and uncertainties in the peak-shape fitting procedures.

Calculations of the Coulomb-excitation cross sections to extract the transition matrix elements from the experimental data were performed using the semiclassical $E2$ coupled-channels code of Winther and de Boer²⁴ which has been expanded to include $E1$, $E3$, and $E4$ excitations. We have performed the calculations in the rigid-rotor limit, which is applicable for a pure rotational spectrum, and included all possible reduced $E2$ and $E4$ matrix elements which connect the 0^+ , 2^+ , 4^+ , and 6^+ members of the ground-state rotational band. In the rigid-rotor limit the intraband matrix elements are given by

$$\begin{aligned} M_{if}(E\lambda) &\equiv \langle I_f \parallel \mathfrak{M}(E\lambda) \parallel I_i \rangle \\ &= (2I_i + 1)^{1/2} \left(\frac{2\lambda + 1}{16\pi} \right)^{1/2} Q_{\lambda 0} \\ &\quad \times \langle I_i \lambda K 0 \mid I_i \lambda I_f K \rangle, \end{aligned} \quad (1)$$

where $Q_{\lambda 0}$ is the "intrinsic" electric multipole moment of order λ .¹⁶ For $\lambda=2$, the $\mathfrak{M}_{if}(E2)$ values corresponding to a prolate shape are used in the analysis. The reduced transition probability for the transition which connects the ground state

of an even-even nucleus to an excited state with spin $I_f = \lambda$ is given by

$$B(E\lambda, 0 \rightarrow I_f = \lambda) = \left(\frac{2\lambda + 1}{16\pi} \right) Q_{\lambda 0}^2. \quad (2)$$

The electric transition matrix elements and excitation scheme used in our calculations of the Coulomb excitation cross sections are shown in Fig. 3. The transition matrix elements which connect the higher vibrational-like state ($2'^+$, $2''^+$, and 3^-) to members of the ground-state rotational band are also shown. Contributions to the excitation probabilities of states in the ground-state band from virtual excitation of these higher states are discussed in Sec. IV.

The experimental excitation probabilities for the 4^+ states in the Th, U, and Pu isotopes are 6 to 25% larger than the calculated values if only the six $E2$ matrix elements between the 0^+ , 2^+ , 4^+ , and 6^+ states are included in the analyses. These experimental excitation probabilities for the 2^+ and 4^+ states are given in Table I. The excess excitation of the 4^+ state is attributed to the presence of $E4$ Coulomb excitation. The influence of the $E4$ matrix elements on the Coulomb-excitation cross section for the 4^+ state in ^{234}U is displayed in Fig. 4 as a function of the reduced $E4$ matrix element $\langle 4 \parallel \mathfrak{M}(E4) \parallel 0 \rangle$.

The quantum mechanical corrections to the excitation probabilities which are obtained from the semiclassical treatment of multiple Coulomb excitation are significant with regard to the deter-

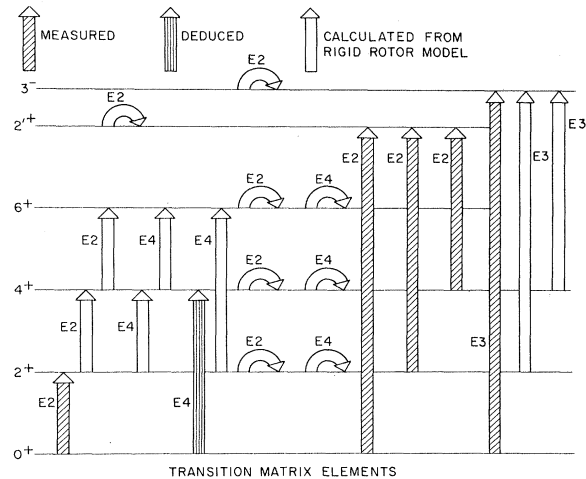


FIG. 3. Electric transition matrix elements included in the calculation of the Coulomb-excitation cross sections in this work. The $2^+ \rightarrow 2'^+$, $4^+ \rightarrow 2'^+$ matrix elements were calculated in the rotational limit relative to the $0^+ \rightarrow 2'^+$ matrix element for all cases except ^{232}Th and ^{238}U . The measured values of Ref. 28 were used for these two cases as indicated in the figure.

TABLE I. Experimental excitation probabilities for the ground-state band with ^4He ions at a laboratory scattering angle of 150° .

Target	E_α (MeV)	$\sigma(2^+)/\sigma(0^+)$	$10^3[\sigma(4^+)/\sigma(0^+)]$	$\frac{[\sigma(4^+)/\sigma(0^+)]_{\text{exp}}}{[\sigma(4^+)/\sigma(0^+)]_{M_{04}(E4)=0}}$
^{230}Th	16.00	0.0869 ± 0.0007	1.59 ± 0.06	1.24 ± 0.05
	17.06	0.1054 ± 0.0008	2.32 ± 0.14	1.23 ± 0.08
^{232}Th	16.00	0.0996 ± 0.0006	2.08 ± 0.08	1.22 ± 0.05
	17.00	0.1201 ± 0.0009	3.06 ± 0.08	1.23 ± 0.04
^{234}U	17.00	0.1303 ± 0.0025	3.65 ± 0.16	1.25 ± 0.07
^{236}U	16.00	0.1165 ± 0.0009	2.73 ± 0.10	1.17 ± 0.05
	17.00	0.1391 ± 0.0013	3.88 ± 0.16	1.17 ± 0.05
^{238}U	16.00	0.1236 ± 0.0008	2.81 ± 0.07	1.08 ± 0.03
	17.00	0.1490 ± 0.0012	3.94 ± 0.14	1.05 ± 0.04
	18.00	0.1726 ± 0.0017	5.60 ± 0.20	1.09 ± 0.04
^{238}Pu	17.00	0.1401 ± 0.0012	3.94 ± 0.15	1.17 ± 0.05
^{240}Pu	17.00	0.1485 ± 0.0015	4.22 ± 0.14	1.11 ± 0.04
^{242}Pu	17.00	0.1504 ± 0.0015	4.09 ± 0.12	1.06 ± 0.04
^{244}Pu	17.00	0.1526 ± 0.0020	4.01 ± 0.17	1.02 ± 0.05
^{244}Cm	17.00	0.1503 ± 0.0018	3.75 ± 0.12	0.98 ± 0.04
^{246}Cm	17.00	0.1543 ± 0.0016	3.95 ± 0.13	0.98 ± 0.04
^{248}Cm	17.00	0.1549 ± 0.0016	4.02 ± 0.14	0.99 ± 0.04

mination of the reduced $E4$ matrix element $\langle 4 || \mathfrak{M}(E4) || 0 \rangle$. The symmetrization of the parameters introduced in the Winther-de Boer computer program²⁴ leads to results which are in very close agreement with the results of a quantum mechanical description of the first-order Coulomb excitation, i.e., direct $E\lambda$ excitation. Alder, Roesel, and Morf²⁵ have investigated the quantum mechanical corrections of the Coulomb-excitation process in second-order perturbation theory and have tabulated the second-order probabilities for a num-

ber of special cases. For the conditions of our experiments the excitation of the 4^+ state is predominantly by the double $E2$ excitation process under the condition $\langle 4 || \mathfrak{M}(E4) || 0 \rangle = 0$. Thus, the use of quantum mechanical corrections from second-order perturbation theory for the $E2$ excitation processes is justified. This correction from the calculations of Alder, Roesel, and Morf²⁵ reduces the excitation probability for the 4^+ state by the pure double $E2$ process by approximately 3% for all of the cases in this paper (varies from 3.16% for ^{230}Th to 2.73% for ^{246}Cm). In Table I the double ratios $[\sigma(4^+)/\sigma(0^+)]_{\text{exp}}/[\sigma(4^+)/\sigma(0^+)]_{M_{04}(E4)=0}$ include this quantum mechanical correction for the double $E2$ excitation.

The experimental results for the reduced transition probabilities $B(E\lambda, 0 \rightarrow I = \lambda)$ and the reduced $E4$ matrix element $M_{04}(E4)$ are summarized in Table II. These results were deduced from the analysis with all seven reduced $E4$ matrix elements $M_{if}(E4)$ included in the multiple Coulomb-excitation calculations. The use of reduced $E4$ matrix elements based on the rigid-rotor model seems justified because the $B(E4, 0 \rightarrow 4)$ values in Table II are very large [$\sim 100 B(E4)_{\text{sp}}$] for the Th, U, and Pu isotopes. The errors associated with $M_{04}(E4)$ values are due principally to uncertainties in the excitation probabilities and $B(E2, 0 \rightarrow 2)$ values. The errors for $M_{04}(E4)$ from an uncertainty in the beam energy and scattering angle are entirely negligible. For example, uncertainties of ± 50 keV in beam energy and $\pm 1^\circ$ in scattering angle introduce errors of $\pm 0.6\%$ and $\pm 0.25\%$, respectively, in $M_{04}(E4)$. However, these uncertain-

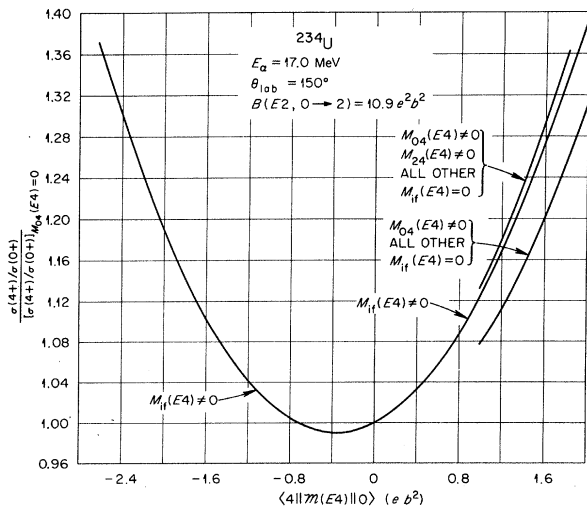


FIG. 4. Influence of the $E4$ matrix elements on the Coulomb-excitation cross section for the 4^+ state in ^{234}U as a function of the reduced $E4$ matrix element $\langle 4 || \mathfrak{M}(E4) || 0 \rangle$.

ties in beam energy and scattering angle do introduce an appreciable uncertainty ($\pm 3\%$) in the $B(E2, 0 \rightarrow 2)$ values. For ^{244}Pu and $^{244-248}\text{Cm}$ the observed 4^+ excitation probabilities are within the experimental errors consistent with that expected from only multiple $E2$ excitation, i.e., without any $E4$ excitation contribution. The limits for $M_{04}(E4)$ given in Table II for these cases are based on the functional dependence of $\sigma(4^+)$ on $M_{04}(E4)$ to the right of its minimum (see for instance Fig. 4). For the other cases we selected the positive solution for $M_{04}(E4)$ because this choice of sign leads to β_{40} deformation parameters that are positive for the Th, U, and Pu isotopes which are in agreement with theoretical calculations.¹⁻³

IV. DISCUSSION OF RESULTS

Several effects, in addition to those mentioned in Sec. III, which could have an influence on the results extracted from the excitation probabilities of the 2^+ and 4^+ states are considered in this section, viz: (A) deviations of $M_{if}(E2)$ from the rigid-rotor limit; (B) higher-order quantal corrections; (C) contributions from virtual excitation of higher states; and (D) interference between Coulomb and direct nuclear excitations.

A. Deviations of $M_{if}(E2)$ from Rigid-Rotor Limit

In the extraction of the $E\lambda$ matrix elements, $\langle 2 || \mathfrak{M}(E2) || 0 \rangle$ and $\langle 4 || \mathfrak{M}(E4) || 0 \rangle$, from the experimental excitation probabilities of the 2^+ and 4^+

states, the rigid-rotor limit relationships given by Eq. (1) were used to generate all other $E2$ and $E4$ intraband matrix elements necessary for the calculation of the Coulomb-excitation probabilities. It is well known that small deviations from the $I(I+1)$ spacings of the level energies of the first few rotational states of the even- A actinide nuclei do exist. Possible mechanisms responsible for these departures could be centrifugal stretching and first-order band mixing from other higher-energy states. For the first few rotational states the level energies are reasonably well described by

$$E(I) = AI(I+1) - BI^2(I+1)^2, \quad (3)$$

where B/A is a measure of the deviation from a rotational level spectrum.

We have considered the effect of deviations of this type by taking the extreme point of view that all of the departure from the $I(I+1)$ spacing is attributable to centrifugal stretching which will then modify the $E2$ matrix elements as follows²⁶:

$$\begin{aligned} \langle I_f || \mathfrak{M}(E2) || I_i \rangle &= (2I_i + 1)^{1/2} \langle I_i 200 | I_i 2I_f 0 \rangle \\ &\times \frac{1 + (B/2A)[I_i(I_i + 1) + I_f(I_f + 1)]}{1 + 3B/A} \\ &\times \langle 2 || \mathfrak{M}(E2) || 0 \rangle. \end{aligned} \quad (4)$$

In the even-even actinide nuclei studied here, the largest deviation²⁷ from a pure rotational spectrum occurs for ^{230}Th where $B/A = 1.31 \times 10^{-3}$. The B/A values for the other cases studied are significantly smaller²⁷ ($0.40 \times 10^{-3} \leq B/A \leq 0.8 \times 10^{-3}$). In this extreme viewpoint, the measured

TABLE II. Experimental results for $B(E\lambda, 0 \rightarrow I = \lambda)$ and $M_{04}(E4)$.

Nucleus	$B(E2, 0 \rightarrow 2)$ ($e^2 \text{b}^2$)	$B(2)/B(E2)_{\text{sp}}^a$	$B(E4, 0 \rightarrow 4)$ ($e^2 \text{b}^4$)	$B(E4)/B(E4)_{\text{sp}}^a$	$M_{04}(E4)$ ($e \text{b}^2$)
^{230}Th	8.06 ± 0.11	193	1.19 ± 0.32	106	1.09 ± 0.15
^{232}Th	9.21 ± 0.09	217	1.48 ± 0.34	129	1.22 ± 0.15
^{234}U	10.90 ± 0.10	256	1.96 ± 0.56	167	1.40 ± 0.20
^{236}U	11.60 ± 0.15	268	1.69 ± 0.57	140	1.30 ± 0.22
^{238}U	12.30 ± 0.15	281	0.69 ± 0.37	56	0.83 ± 0.22
^{238}Pu	12.63 ± 0.17	288	1.90 ± 0.67	154	1.38 ± 0.25
^{240}Pu	13.33 ± 0.18	301	1.31 ± 0.62	104	1.15 ± 0.28
^{242}Pu	13.47 ± 0.18	301	$0.55_{-0.41}^{+0.53}$	43	0.74 ± 0.34
^{244}Pu	13.61 ± 0.18	301	$0.09_{-0.08}^{+0.55}$	7	$0.03_{-0.5}^{+0.5}$
^{244}Cm	14.58 ± 0.19	322	$0.0_{-0.0}^{+0.25}$	0	$0.0_{-0.5}^{+0.3}$
^{246}Cm	14.94 ± 0.19	326	$0.0_{-0.0}^{+0.25}$	0	$0.0_{-0.5}^{+0.3}$
^{248}Cm	14.99 ± 0.19	324	$0.0_{-0.0}^{+0.36}$	0	$0.0_{-0.5}^{+0.5}$

^a $B(E\lambda)_{\text{sp}} = (2\lambda + 1/4\pi)(3/\lambda + 3)^2 (0.12A^{1/3})^{2\lambda} e^2 \text{b}^\lambda$ for $I_i = 0, I_f = \lambda$.

value of $\langle 4 \parallel \mathfrak{M}(E4) \parallel 0 \rangle$ for ^{230}Th would be reduced by 7.9% compared to our quoted experimental uncertainty of 14%. The use of the rigid-rotor relationships, therefore, for the intraband $E2$ and $E4$ matrix elements is a good assumption in light of the small effect of the measured $\langle 4 \parallel \mathfrak{M}(E4) \parallel 0 \rangle$ values.

B. Higher-Order Quantal Corrections

We have included the quantum mechanical corrections to the calculated semiclassical multiple $E2$ excitation probabilities for the 2^+ and 4^+ states as discussed in Sec. III. The quantal correction to the calculated 4^+ excitation probability for pure double $E2$ excitation and a simultaneous direct $E4$ excitation in first order, would be $\sim +0.5\%$ for the cases studied here. The net effect of a $+0.5\%$ correction in the calculated 4^+ excitation probability due to this process would be to reduce the measured $E4$ matrix elements $\langle 4 \parallel \mathfrak{M}(E4) \parallel 0 \rangle$ by 1.8% for a case such as ^{234}U . This correction has not been included in the analysis of the data for the actinide nuclei because higher-order effects for these cases are more important; e.g., compare the calculations for the case $M_{04}(E4) \neq 0$ and all other $M_{if}(E4) = 0$ with the case $M_{if}(E4) \neq 0$ in Fig. 4. The quantal corrections for the higher-order $E4$ excitations are not available. It is possible that the quantal corrections for these higher-order effects could have a significant influence on the extraction of the reduced $E4$ matrix elements from experimental data. There is thus a distinct need for theoretical studies of the quantal corrections for higher-order excitation processes.

C. Contributions from Virtual Excitation of Higher States

To test the influence of virtual excitation of higher excited states on the excitation probabilities of the 2^+ and 4^+ states in the ground-state rotational band requires a knowledge of the interband $E\lambda$ matrix elements which connect these states. For ^{232}Th and ^{238}U the magnitude of most of the $E\lambda$ matrix elements are available from the analysis of γ -ray spectroscopy of the Coulomb excitation reaction.²⁸ For the other actinide nuclei in this paper, we have been able to extract, from the inelastically scattered ^4He ion spectra, $E\lambda$ matrix elements for 2 or 3 higher excited states resulting primarily from direct $E2$ and $E3$ Coulomb excitation. The influence of the virtual excitation of higher states on the extracted $B(E2, 0 \rightarrow 2)$ and $M_{04}(E4)$ is given in Table III. Column 2 contains spins and parities of the higher states included in the calculations. The signs of

interband $E\lambda$ matrix elements were chosen according to the Bohr-Mottelson collective model with the intrinsic transition matrix elements taken from the experimental $B(E2, 0 \rightarrow 2')$, $B(E2, 0 \rightarrow 2'')$, and $B(E3, 0 \rightarrow 3)$ values.^{22, 28} The contributions from the inclusion of the higher states in the analysis are very small and depend to some extent on the type and number of states included in the calculations. In view of these points and of the model dependence for the choice of signs for the interband $E\lambda$ matrix elements, we have not included the higher states in the analyses for the results presented in Table II.

Contributions to the excitation probability of the 2^+ state due to virtual excitation of states in the giant dipole resonance are negligibly small ($\sim -0.1\%$). For this estimate of the influence of virtual excitation, we have used the energy-weighted sum rule²⁹ to obtain values for $B(E1, 0 \rightarrow 1^-)$ and the result $\langle 2^+ \parallel \mathfrak{M}(E1) \parallel 1^- \rangle / \langle 0^+ \parallel \mathfrak{M}(E1) \parallel 1^- \rangle \approx \frac{1}{12}$ from a calculation by MacDonald.³⁰

D. Interference Between Coulomb and Direct Nuclear Excitations

The validity of the semiclassical treatment of Coulomb excitation as used in the analyses of our experimental data depends on the complete absence of direct nuclear reactions. Coulomb excitation is the only reaction which can take place if the bombarding energy is sufficiently low so that the projectile does not penetrate into the range of nuclear forces. For our typical experimental conditions, 17-MeV ^4He ions on ^{238}U and a scattering angle of 150° , the distance of closest approach is 16.4 fm. If we make the (incorrect) assumption that the nuclei are spherical, the separation distance S between the two nuclear surfaces at the point of closest approach is about 7 fm for a nuclear radius $R = r_0 A^{1/3}$ and $r_0 = 1.2$ fm. At the present time experimental evidence from the analysis^{31, 32} of Coulomb-excitation experiments designed to measure static quadrupole moments suggests that S should be at least 5 fm and possibly as large as 6 fm to insure pure Coulomb excitation with heavy ions. For ^4He ions the safe-bombardment-energy prescription of Cline³¹ corresponds to a minimum distance of closest approach of 16 fm at a scattering angle of 180° . Furthermore, measurements by Barnett and Phillips³³ of the very small cross sections for Coulomb excitation of the 3^- state in ^{208}Pb show that Coulomb excitation is the dominant process at ^4He energies of 17.5 and 18 MeV, although direct nuclear reactions are evident at 19 MeV. Translating this information on ^{208}Pb to the actinide nuclei indicates that 17-, 18-, or even 19-MeV ^4He

TABLE III. Influence of the virtual excitation of higher states on the extracted $B(E2, 0 \rightarrow 2)$ and $M_{04}(E4)$. Column 2 lists spin and parity of the higher states included in the calculations.

Nucleus	I^π of higher states	$\Delta B(E2)/B(E2, 0 \rightarrow 2)$ (%) ^a	$\Delta M_{04}(E4)/M_{04}(E4)$ (%) ^a
²³⁰ Th	$3^-, 2'^+, 2''^+$	-0.3	-2.0
²³² Th	$0'^+, 2'^+, 3^-, 2''^+, 4'^+, 3^-$	0.0	-4.0
²³⁴ U	$3^-, 2'^+, 2''^+$	-0.2	0.0
²³⁶ U	$3^-, 2'^+$	-0.1	-1.0
²³⁸ U	$3^-, 2'^+$	-0.2	-2.3
²³⁸ Pu	$3^-, 2'^+$	-0.1	-1.9
²⁴⁰ Pu	3^-	0.0	-2.3
²⁴² Pu	$3^-, 3^-, 2'^+$	-0.1	-6.0
²⁴⁴ Pu	$3^-, 3^-, 2'^+, 2''^+$	-0.1	...
²⁴⁴ Cm	$3^-, 3^-, 2'^+$	0.0	...
²⁴⁶ Cm	$2'^+, 3^-$	0.0	...
²⁴⁸ Cm	$3^-, 3^-$	-0.1	...

^a Net change in $B(E2, 0 \rightarrow 2)$ and $M_{04}(E4)$ resulting from the inclusion of all of the states listed in column 2.

ions should be safe energies for Coulomb excitation. Since we are dealing with target nuclei with rather large static deformations, it is not clear that these prescriptions for safe bombarding energies apply. As a result the excitation probabilities for the 2^+ and 4^+ states in ²³⁴U were measured at

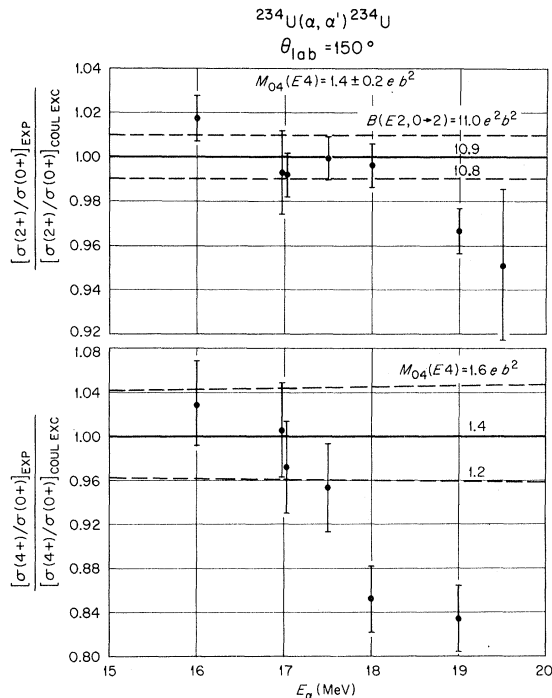


FIG. 5. Experimental excitation probabilities for the 2^+ and 4^+ states in ²³⁴U relative to the elastic scattering as a function of bombarding energy. The results are presented in units of the probabilities for pure Coulomb excitation with $B(E2, 0 \rightarrow 2) = 10.9 e^2 b^2$ and $M_{04}(E4) = 1.4 e b^2$.

incident energies between 16 and 19.5 MeV.

The experimental excitation probabilities for the 2^+ and 4^+ states relative to the elastic scattering are shown in Fig. 5 as a function of bombarding energy. The experimental results are presented in units of the probabilities for pure Coulomb excitation with $B(E2, 0 \rightarrow 2) = 10.9 \pm 0.1 e^2 b^2$ and $M_{04}(E4) = 1.4 \pm 0.2 e b^2$ at a scattering angle of 150° . Calculation of the Coulomb-excitation probabilities was done in the limit of the rigid-rotor model with states 0^+ , 2^+ , 4^+ , and 6^+ and included quantum mechanical corrections taken from second-order perturbation theory.²⁵ The 2^+ excitation probability begins to show a deviation from the prediction of pure Coulomb excitation at 19 MeV. For the 4^+ excitation probability, however, a marked deviation begins at 18 MeV. Both excitation probabilities show the destructive interference expected between Coulomb and direct nuclear excitations. The $M_{if}(E\lambda)$ used in the calculation of the pure-Coulomb-excitation probabilities were extracted from the experimental data at 16, 17, and 17.5 MeV for $B(E2, 0 \rightarrow 2)$ and at 16 and 17 MeV for $M_{04}(E4)$. The onset of the destructive interference structure occurs at a lower bombarding energy for the 4^+ excitation than for the 2^+ excitation and the deviation from pure Coulomb excitation is larger for the 4^+ excitation. In any case, the safe-bombardment-energy prescription given above is inadequate to insure pure Coulomb excitation of the actinide nuclei with ⁴He ions. The $M_{04}(E4)$ extracted from the 4^+ excitation probabilities at the various bombarding energies are shown in Fig. 6 on the assumption of pure Coulomb excitation at each energy. The solid data points are based on the $B(E2, 0 \rightarrow 2)$ extracted from the 2^+ excitation probability at the corres-

ponding bombarding energy. The $M_{04}(E4)$ extracted on the basis of $B(E2, 0 \rightarrow 2) = 10.9 e^2 b^2$ are denoted by open-circle data points. Since the destructive interference structure does not occur at the same energy for the 2^+ and 4^+ excitations, one could obtain rather erroneous and erratic results from $M_{04}(E4)$ extracted from measurements taken at an unsafe bombarding energy and assuming only pure-Coulomb-excitation processes.

The measurements at $E_\alpha = 16$ and 17 MeV of the excitation probabilities (see Table I) for the 2^+ and 4^+ states of the ground-state band in ^{238}U and ^{236}U indicate that the destructive interference at 17 MeV between Coulomb and direct nuclear excitations is sufficiently small and does not influence the results deduced from the excitation probabilities. However, the experimental results for $B(E2, 0 \rightarrow 2)$ and $M_{04}(E4)$ in Table II for ^{238}U are different from the values published by us in an earlier communication¹⁵ in which the excitation probabilities were measured at $E_\alpha = 18$ MeV. The $B(E2, 0 \rightarrow 2)$ deduced from the 2^+ excitation prob-

ability at $E_\alpha = 18$ MeV in Table I is $11.90 \pm 0.15 e^2 b^2$, whereas the $B(E2, 0 \rightarrow 2)$ deduced from the measurement at $E_\alpha = 16$ or 17 MeV is $12.30 \pm 0.15 e^2 b^2$. Therefore, the value of $M_{04}(E4)$ for ^{238}U quoted in the earlier communication¹⁵ must be corrected because of the interference between Coulomb and direct nuclear excitations. The new result $M_{04}(E4) = 0.83 \pm 0.22$ deduced from the measurement at $E_\alpha = 16$ MeV is significantly smaller than the earlier result.¹⁵

V. DEFORMATION PARAMETERS

A. Extraction of Deformation Parameters

The large transition moments observed in the ground-state rotational band suggests that these moments arise from the intrinsic shape of the deformed nuclei. Model-dependent deformation parameters, β_{20} and β_{40} , have been extracted from the measured $E2$ and $E4$ transition moments for distributions of nuclear charge represented by a deformed homogeneous distribution and by several forms of the Fermi distribution for deformed nuclei by solving the equations for the volume integral

$$\langle I_f = \lambda \| 3\mathcal{M}(E\lambda) \| 0 \rangle = \int r^\lambda Y_{\lambda 0}(\theta) \rho(r, \theta) dr \quad (5)$$

numerically. The charge distribution function is $\rho(r, \theta)$.

For a deformed homogeneous distribution of nuclear charge with a surface defined by

$$R(\theta) = R_0 [1 + \beta_{20} Y_{20}(\theta) + \beta_{40} Y_{40}(\theta)],$$

we have

$$\rho(r, \theta) = \rho_0 \quad \text{for } r \leq R(\theta),$$

and

$$\rho(r, \theta) = 0 \quad \text{for } r > R(\theta). \quad (6)$$

The deformation parameters, β_{20} and β_{40} , were varied in an iteration procedure to produce the measured $M_{02}(E2)$ and $M_{04}(E4)$ matrix elements. The charge density ρ_0 was held constant at the value which it would have for zero deformation, i.e., $\rho_0 = 3Ze/4\pi(r_0 A^{1/3})^3$ with $r_0 = 1.2$ fm. The parameter $R_0 = r_0 A^{1/3}$ was adjusted slightly for the deformed shape in order to conserve the total nuclear charge. This adjustment for R_0 ranged between 0.27% for ^{230}Th and 0.12% for ^{248}Cm . The results obtained for β_{20} and β_{40} are summarized in Table IV.

The use of a Fermi-type charge distribution has been quite successful in the analysis of data from electron scattering and muonic x-ray spectra for spherical nuclei. For deformed nuclei, the Fermi distribution of nuclear charge has been extended

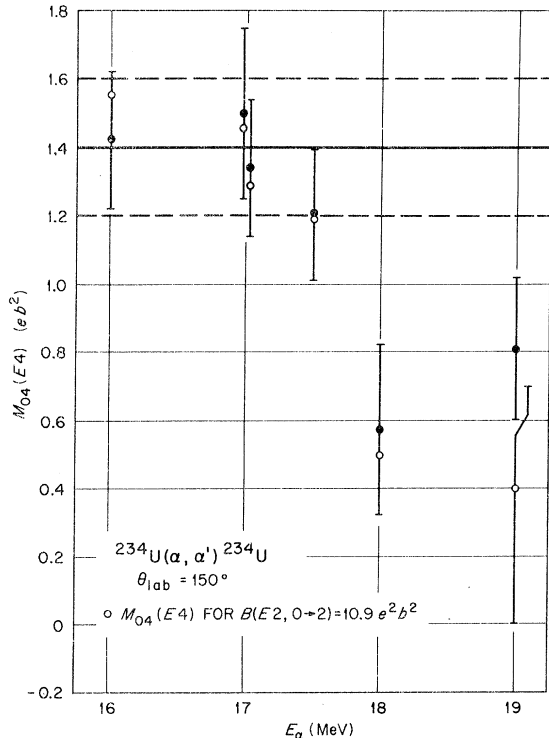


FIG. 6. $M_{04}(E4)$ extracted from the 4^+ excitation probabilities at the various bombarding energies for ^{234}U on the assumption of pure Coulomb excitation at each energy. The solid points are based on the $B(E2, 0 \rightarrow 2)$ extracted from the 2^+ excitation probability at the corresponding bombarding energy. $M_{04}(E4)$ extracted on the basis of $B(E2, 0 \rightarrow 2) = 10.9 e^2 b^2$ are denoted by open circle data points.

TABLE IV. Quadrupole and hexadecapole deformations.

Nucleus	Homogeneous distribution ^a		Deformed Fermi distribution (Modified c) ^b		Harmonic-oscillator potential ^c		Woods-Saxon potential ^d	
	β_{20}	β_{40}	β_{20}	β_{40}	β_{20}	β_{40}	β_{20}	β_{40}
²³⁰ Th	0.204 ± 0.005	0.104 ± 0.018	0.227 ± 0.006	0.119 ± 0.021	0.191	0.087	0.195	0.092
²³² Th	0.214 ± 0.005	0.113 ± 0.018	0.238 ± 0.006	0.130 ± 0.020	0.206	0.084	0.206	0.084
²³⁴ U	0.223 ± 0.006	0.123 ± 0.022	0.248 ± 0.007	0.142 ± 0.026	0.205	0.079	0.210	0.085
²³⁶ U	0.232 ± 0.007	0.108 ± 0.025	0.259 ± 0.008	0.124 ± 0.028	0.214	0.073	0.219	0.075
²³⁸ U	0.253 ± 0.007	0.051 ± 0.025	0.283 ± 0.008	0.059 ± 0.029	0.222	0.065	0.228	0.063
²³⁸ Pu	0.235 ± 0.008	0.110 ± 0.027	0.262 ± 0.009	0.127 ± 0.031	0.222	0.072	0.223	0.070
²⁴⁰ Pu	0.248 ± 0.008	0.082 ± 0.030	0.277 ± 0.010	0.094 ± 0.035	0.229	0.064	0.233	0.059
²⁴² Pu	0.260 ± 0.010	0.036 ± 0.037	0.292 ± 0.012	0.041 ± 0.043	0.234	0.055	0.240	0.048
²⁴⁴ Pu	0.272 ± 0.018	-0.013 ± 0.073	0.307 ± 0.022	-0.016 ± 0.085	0.242	0.047	0.247	0.038
²⁴⁴ Cm	0.284 ± 0.011	-0.048 ± 0.045	0.321 ± 0.013	-0.057 ± 0.052	0.241	0.052	0.242	0.040
²⁴⁶ Cm	0.286 ± 0.011	-0.094 ± 0.044	0.324 ± 0.013	-0.057 ± 0.052	0.248	0.044	0.245	0.030
²⁴⁸ Cm	0.285 ± 0.014	-0.049 ± 0.060	0.323 ± 0.018	-0.057 ± 0.070	0.246	0.032	0.246	0.020

^a Calculated for $r_0 = 1.2$ fm.^b Calculated using $c_0 = 1.10$ fm and $a = 0.5$ fm.^c Nilsson *et al.* (Ref. 1).^d Alder *et al.* (Ref. 3).

in several ways although there is no unique way to introduce deformation for the treatment of muonic x-ray data.³⁴ A generalization of the Fermi distribution for deformed nuclei is as follows:

$$\rho(r, \theta) = \rho_0 / (e^x + 1), \quad (7)$$

where

$$x = \frac{r - c(1 + \beta_{20}Y_{20} + \beta_{40}Y_{40})}{a(1 + \beta_{20}\gamma_2Y_{20} + \beta_{40}\gamma_4Y_{40})}.$$

In Eq. (7) c is the half-density radius and a is the diffuseness parameter which is related to the surface thickness t , the radial distance between 90 and 10% densities, by $t = 4a \ln 3$. To make a distinction between half-density radius c and the parameter R_0 for the homogeneous distribution we write $c = c_0 A^{1/3}$. The shape parameters γ_2 and γ_4 influence the distribution of quadrupole and hexadecapole charge within the nucleus and also serve to distinguish the three models which have been considered in the analysis of muonic x-ray data for deformed nuclei: viz.

- (a) modified- c distribution: $\gamma_2 = \gamma_4 = 0$;
- (b) deformed-Fermi distribution: $\gamma_2 = \gamma_4 = 1.0$;
- (c) hard-core distribution: $\gamma_2 = \gamma_4 = c/2 \ln 3$ (contour of charge density $\rho = 0.9\rho_0$ is spherical).

The deformation parameters, β_{20} and β_{40} , have been extracted from the measured $E2$ and $E4$ transition moments for these three models of the Fermi-type charge distributions using values³⁴ of the parameters a and c_0 representative of the best fits from the analysis of muonic x-ray data, viz. $c_0 = 1.10$ fm with $a = 0.5$ and 0.6 fm and $c_0 = 1.15$ fm with $a = 0.4$ fm. Again the density ρ_0 was held constant in the numerical calculations at the value which it

would have for zero deformation, i.e.,

$$\rho_0 = Ze / \int \frac{d\tau}{1 + \exp[(r - c_0 A^{1/3})/a]}.$$

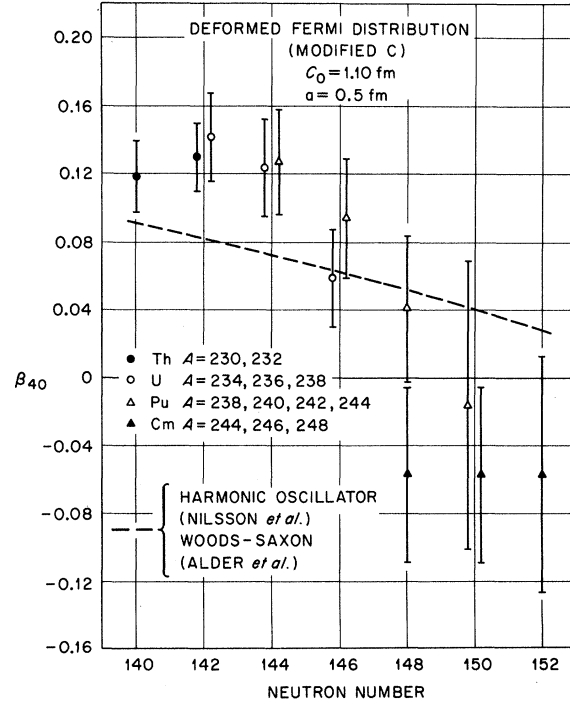


FIG. 7. Hexadecapole deformations β_{40} extracted from the measured $E2$ and $E4$ transition moments for a modified- c Fermi distribution as a function of neutron number. The equilibrium values from the calculations by Nilsson *et al.* and by Alder *et al.* are shown for comparison.

The parameter c_0 was adjusted slightly (-0.4 to -0.9%) for the deformed shape in order to conserve the total nuclear charge. If the extraction of β_{20} and β_{40} is performed with c_0 held constant and ρ_0 adjusted for the deformed shape to conserve the total nuclear charge, very small differences occur in the results for ρ_0 , β_{20} , and β_{40} . For instance, the changes in ρ_0 , β_{20} , and β_{40} for ^{234}U are -1.8 , -0.8 , and -2.0% , respectively, for a modified- c distribution. The quadrupole and hexadecapole deformation parameters β_{20} and β_{40} are listed in Table IV for a modified- c distribution with $c_0 = 1.10$ fm and $a = 0.5$ fm.

In Table IV we have also included the equilibrium deformation parameters which have been calculated on the basis of a modified harmonic-oscillator potential model by Nilsson *et al.*¹ and of a Woods-Saxon potential model by Alder *et al.*³ The connection between the deformation parameters of the potential, ϵ and ϵ_4 , as given by Nilsson *et al.*,¹ and the deformation parameters, β_{20} and β_{40} , defining the nuclear surface, was made by a numerical integration procedure involving the corresponding equations for the radius vector as a function of angle with suitable volume normalization constants.³⁵ The quadrupole deformations β_{20} from the modified- c distribution are 16 to 26% larger than the equilibrium values from the calculations by Nilsson *et al.* and by Alder *et al.*

The hexadecapole deformations β_{40} are rather large for $^{230, 232}\text{Th}$, $^{234, 236}\text{U}$, and $^{238, 240}\text{Pu}$. In Fig. 7 the hexadecapole deformations are displayed as a function of neutron number together with the equilibrium values from the calculations by Nilsson *et al.* and by Alder *et al.* The small differences between the two calculations have been neglected for the purpose of Fig. 7 as well as the slight Z dependence of β_{20} for a given neutron number. The data support the general trend of the calculations with neutron number, namely, that the equilibrium values are large and positive at the beginning of the deformed region, decrease slowly

to zero near $N = 156$ and become negative for $N > 156$. However, the experimental results at $N = 142$ and 144 are ~ 1.7 times larger than the ground-state equilibrium calculations for β_{40} . Alder has pointed out that the exact equilibrium point with respect to β_{40} is not well determined and an uncertainty of 0.01 in β_{40} is possible in the calculations. However, this is small compared to the deviations from the experimental data. The β_{40} from the experimental data for ^{244}Pu and $^{244-248}\text{Cm}$ ($N \geq 148$) are poorly determined because of the weak dependence of the 4^+ excitation probability on values of $M_{04}(E4)$ near zero and slightly negative, i.e., the interference between the $E2$ and $E4$ modes of excitation is destructive (see for instance Fig. 4).

Changes in the extracted equilibrium deformations β_{20} and β_{40} for ^{234}U for different choices of the Fermi charge distribution for deformed nuclei and with and without the inclusion of a finite β_{60} are listed in Table V together with the central charge density ρ_0 and the adjusted values of c_0 to conserve nuclear charge. The inclusion of $\beta_{60} = 0.015$ in the analysis decreases the extracted value of β_{40} by 4.4% . This value of β_{60} is typical of that contained in the shape of the modified harmonic-oscillator potential calculations by Nilsson *et al.*¹ The value of β_{20} is essentially unaltered with the inclusion of $\beta_{60} = 0.015$ in the analysis. The values of β_{20} and β_{40} extracted from the deformed-Fermi and hard-core distributions are significantly smaller. In these two models of the charge distribution the diffuseness parameter as well as the radial parameter are functions of the polar angle θ . Figure 8 shows the lines of constant charge density ($\rho = 0.9\rho_0$, $0.5\rho_0$, and $0.1\rho_0$) with $\gamma_2 = \gamma_4 = 0.0, 1.0$, and 6.17 for the case of ^{234}U . The transition moments, $M_{02}(E2)$ and $M_{04}(E4)$, and the central charge density ρ_0 are the same for these distributions. The analysis³⁶ of muonic x-ray data from deformed nuclei in terms of the charge distributions of the Fermi type which

TABLE V. Changes in the equilibrium deformation β_{20} and β_{40} for different choices of the Fermi charge distribution for deformed nuclei and with the inclusion of a finite β_{60} for ^{234}U . The changes $\Delta\beta_{20}$ and $\Delta\beta_{40}$ are relative to $\beta_{20} = 0.248$ and $\beta_{40} = 0.142$ deduced from a modified- c Fermi distribution with $c_0 = 1.10$ fm and $a = 0.50$ fm.

Type of distribution	c_0 (fm)	a (fm)	c_0 (adjusted) (fm)	ρ_0 (protons/fm ³)	β_{60}	$\Delta\beta_{20}/\beta_{20}$ (%)	$\Delta\beta_{40}/\beta_{40}$ (%)
Modified c	1.10	0.50	1.093	0.0669	0.015	-0.1	-4.4
Deformed	1.10	0.50	1.094	0.0669	0.0	-5.4	-11.9
Hard core	1.10	0.50	1.094	0.0669	0.0	-29.3	-56.2
Modified c	1.10	0.60	1.093	0.0655	0.0	-0.5	-6.5
Modified c	1.10	0.60	1.093	0.0655	0.015	-0.6	-10.7
Modified c	1.15	0.40	1.143	0.0598	0.0	-5.4	-8.5
Modified c	1.15	0.40	1.144	0.0598	0.015	-5.6	-12.8

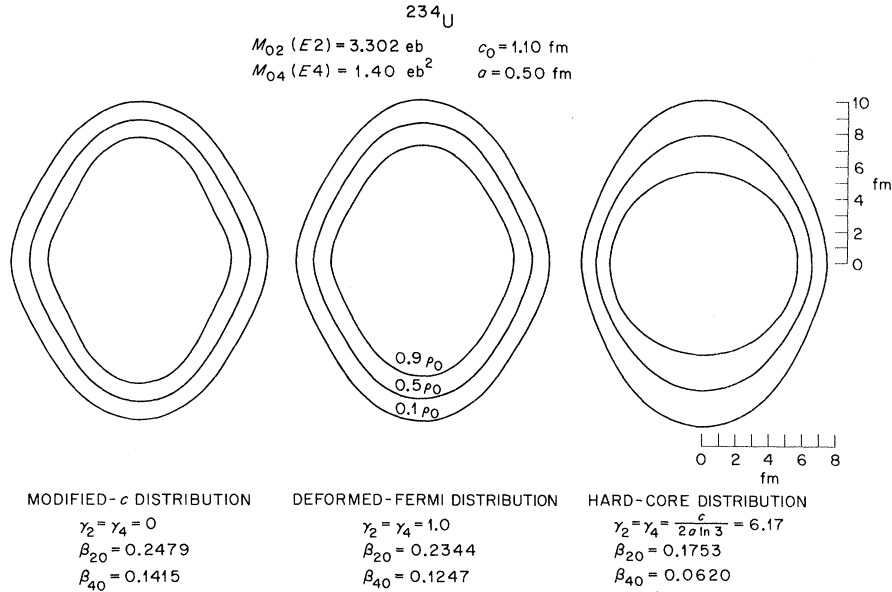


FIG. 8. Lines of constant charge density ($\rho = 0.9\rho_0$, $0.5\rho_0$, and $0.1\rho_0$) for the modified- c , deformed-Fermi, and hard-core distributions of nuclear charge for ^{234}U . The transition moments, $M_{02}(E2)$ and $M_{04}(E4)$, and the central density ρ_0 are the same for these distributions.

includes only the quadrupole deformation β_{20} favors the modified- c and deformed-Fermi models over the hard-core model. It would seem that the analysis of muonic x-ray spectra should possibly include the hexadecapole interaction and the hexadecapole deformation in the models of the deformed Fermi nuclear charge distribution. Although the hexadecapole interaction may be small in muonic x-ray experiments and hence neglected, the quadrupole moment contains contributions from the $\beta_{40}Y_{40}$ component of the shape as well as the $\beta_{20}Y_{20}$ component. For the hard-core distribution in which $\rho = 0.9\rho_0$ is spherically symmetric, the extracted values of β_{40} are smaller than the equilibrium values from the calculations by Nilsson *et al.* and by Alder *et al.* Since this is an extreme choice of the parameters γ_2 and γ_4 in the hard-core distribution, we have extracted the de-

TABLE VI. Equilibrium deformation β_{20} and β_{40} for different choices of γ_2 and γ_4 in the Fermi charge distribution for ^{234}U with $c_0 = 1.10 \text{ fm}$ and $a = 0.50 \text{ fm}$ ($c = 6.778 \text{ fm}$); columns 4 and 5 give the charge-density contour which is spherical and the radius of this contour.

Type of distribution	γ_2	γ_4	Charge-density contour	Radius of contour	β_{20}	β_{40}
Modified c	0.0	0.0			0.248	0.142
Deformed	1.0	1.0	ρ_0	0.0	0.234	0.125
Hard core	2.0	2.0	$0.999\rho_0$	$0.5c$	0.221	0.109
Hard core	3.085	3.085	$0.988\rho_0$	$0.676c$	0.208	0.094
Hard core	4.0	4.0	$0.967\rho_0$	$0.75c$	0.197	0.083
Hard core	6.17	6.17	$0.9\rho_0$	$0.838c$	0.175	0.062

formation parameters β_{20} and β_{40} for other values of γ_2 and γ_4 in the Fermi charge distribution for ^{234}U with $c_0 = 1.10 \text{ fm}$ and $a = 0.50 \text{ fm}$ ($c = 6.778 \text{ fm}$). The results are summarized in Table VI. Columns 4 and 5 give the charge-density contour which is spherical and the radius of this contour. The extracted values of β_{20} and β_{40} are significantly smaller even for the case $\gamma_2 = \gamma_4 = 2.0$ where the radius of the spherical density contour is $0.5c$.

B. Choice of Sign for $\langle 4^+ || \mathfrak{M}(E4) || 0^+ \rangle$

As can be noted from Fig. 4, the dependence of the effect of the $E4$ matrix elements on the 4^+ cross section is double valued for $\langle 4^+ || M(E4) || 0^+ \rangle$. However, the curve is not symmetric about $M_{04}(E4) = 0$ because the net interference between the $E2$ and $E4$ excitation processes is destructive for $M_{04}(E4) < 0$ and constructive for $M_{04}(E4) > 0$. We have chosen to analyze experimental data using the positive solution to $M_{04}(E4)$ because this choice of sign leads to β_{40} deformation parameters that are > 0 for the Th, U, and Pu isotopes which is in agreement with the theoretical calculations¹⁻³ and with other recent experimental results.^{14, 17}

The negative choice for $M_{04}(E4)$ would, in addition to a sign change for β_{40} , lead to considerably larger values for the $E4$ transition probability and also lead to very much larger $|\beta_{40}|$ deformation parameters. For example, in ^{234}U , the $\langle 4^+ || \mathfrak{M}(E4) || 0^+ \rangle$ value would be -2.26 eb^2 and the $B(E4, 0^+ \rightarrow 4^+)$ would have a strength of 435 single-particle units.

The model-dependent deformation parameters in this case would be $\beta_{20} = 0.310 \pm 0.003$ and $\beta_{40} = -(0.353 \pm 0.030)$ for the homogeneous charge distribution and $\beta_{20} = 0.358 \pm 0.004$ and $\beta_{40} = -(0.413 \pm 0.036)$ for the modified- c Fermi distribution with $c_0 = 1.1$ fm and $a = 0.5$ fm. The magnitude of these deformation parameters makes the choice of $M_{04}(E4) < 0$ for ^{234}U unlikely.

Multiple-Coulomb-excitation experiments with heavy ions performed at Oak Ridge by Eichler *et al.*³⁷ also support our choice of sign for $M_{04}(E4)$. In these experiments, the ground-state rotational bands of ^{232}Th and ^{238}U have been excited up to the 12^+ or 14^+ state. Analyses of the excitation probabilities for the higher-spin states of the ground-state band, first with only $E2$ matrix elements, and then including the $E4$ matrix elements for both the positive and negative solution, support our choice of sign for $M_{04}(E4)$. Deviations as large as 30 to 70% from the experimental probabilities for the 8^+ , 10^+ , and 12^+ states were noticed when the negative solution for $M_{04}(E4)$ was used, while the positive solution for $M_{04}(E4)$ yielded excitation probabilities in agreement with experiment.

C. Comparison with Other Results

As pointed out by Satchler,³⁸ caution must be used when comparisons are made between deformations of the nuclear charge as obtained in electromagnetic measurements and deformations of the nuclear potential which are derived from inelastic scattering experiments at energies above the Coulomb barrier. To the extent that such a comparison may be made, we have compared the charge-deformation parameters derived from our experiments with the potential deformation parameters derived from the (p, p') experiments of Moss *et al.*¹⁴ for ^{232}Th and ^{238}U and from the (α, α') experiments of Hendrie *et al.*¹⁷ for ^{238}U . This com-

parison is given in Table VII where we have included both our charge deformations for the homogeneous distribution ($r_0 = 1.2$ fm) and for the modified- c Fermi distribution with $c_0 = 1.10$ fm and $a = 0.5$ fm. It is noted that reasonable agreement for β_{20} is achieved between the Coulomb-excitation results based on the modified- c Fermi distribution and the (p, p') results of Moss *et al.* but the hexadecapole deformations from Coulomb excitation are about 2.5 times larger. The β_{20} deformation for ^{238}U from the (α, α') measurements of Hendrie *et al.* is $\sim 20\%$ smaller than our Coulomb-excitation results but the β_{40} deformations are in agreement. A more meaningful comparison between these two types of experiments, both of which yield valuable information about the static nuclear shape, will have to await further theoretical development. A comparison of transition moments rather than deformation parameters, would avoid the problem of model-dependent nuclear shapes.

Mössbauer experiments have also been performed in the actinide region by Monard *et al.*³⁹ and by Meeker *et al.*⁴⁰ In these experiments, the intrinsic quadrupole moment ratios for the isotopes ^{234}U , ^{236}U , and ^{238}U have been determined. Monard³⁹ obtains values for the ratio $Q_{234} : Q_{236} : Q_{238}$ of $1.0 : 0.98 \pm 0.05 : 1.10 \pm 0.07$, while Meeker *et al.*⁴⁰ have determined values of $1.0 : 1.08 \pm 0.04 : 1.08 \pm 0.06$. Both of these data, within their experimental errors, agree with our present values of $1.0 : 1.032 \pm 0.016 : 1.062 \pm 0.016$ which show an almost linear increase with mass number. Monard³⁹ has also attempted to observe the hexadecapole interaction in Mössbauer experiments with ^{234}U but concluded other effects were more important in their analyses.

Recent measurements of the lifetimes of excited 2^+ and 4^+ rotational states in some of the actinides by Ton *et al.*⁴¹ have yielded $B(E2)$ values in agreement with our values.

TABLE VII. Comparison of deformation parameters deduced from Coulomb excitation and from inelastic scattering at bombarding energies well above the Coulomb barrier.

		Coulomb excitation			
		Uniform distribution $r_0 = 1.2$ fm	Deformed Fermi distribution ^a	(p, p') ^b	(α, α') ^c
^{232}Th	β_{20}	0.214 ± 0.005	0.238 ± 0.006	0.23 ± 0.01	
	β_{40}	0.113 ± 0.018	0.130 ± 0.020	0.050 ± 0.015	
	β_{60}	
^{238}U	β_{20}	0.253 ± 0.007	0.283 ± 0.008	0.27 ± 0.01	0.22 ± 0.01
	β_{40}	0.051 ± 0.025	0.059 ± 0.029	$0.017^{+0.015}_{-0.030}$	0.06 ± 0.01
	β_{60}	-0.015	-0.012 ± 0.01

^a Modified- c distribution with $c_0 = 1.10$ fm and $a = 0.50$ fm.

^b Moss *et al.* (Ref. 14); scaled for $r_0 = 1.2$ fm.

^c Hendrie *et al.* (Ref. 17); scaled for $r_0 = 1.2$ fm.

Braid *et al.*⁴² in their studies of the neutron single-particle states in the U, Pu, and Cm isotopes are able to place reasonable bounds on the equilibrium deformation parameters from the extracted single-particle spectrum. Using a momentum-dependent Woods-Saxon potential⁴³ to investigate the changes in level spectrum with changes in deformation parameters, these authors report that with $\beta_2 = 0.24 \pm 0.01$, $\beta_4 = 0.00 \pm 0.01$, and $\beta_6 = 0.01 \pm 0.01$, a reasonable fit to the data is achieved. We concur that the hexadecapole deformation parameter, β_4 , is nearly zero for $A \geq 242$ based either on the homogeneous or Fermi distributions and perhaps becomes slightly negative for $A \sim 246$. However, the quadrupole deformations β_2 , derived from our results are significantly larger than $\beta_2 = 0.24$ as reported by Braid *et al.*⁴²

VI. CONCLUSIONS

We have demonstrated that substantial electric hexadecapole transition moments exist in the actinide deformed region, particularly for the Th, U, and lighter Pu nuclei and that by the inclusion of the hexadecapole deformation, a very important contribution to the description of the charge deformation of the nuclear surfaces is made. Coulomb excitation with lighter ions such as ^4He has been demonstrated to be an effective and useful probe of the quadrupole and hexadecapole com-

ponents of the nuclear charge distribution. Since multiple excitations with ^4He ions are minimized, as contrasted to the heavy ions ^{16}O , ^{20}Ne , and ^{40}Ar , etc., the experiments are relatively simple to interpret and since Coulomb excitation is a pure electromagnetic interaction, the experimental results may be interpreted quantitatively. It is clear, that further theoretical interpretation is required before a meaningful comparison may be made between charge deformations inferred from Coulomb-excitation experiments and the potential deformations inferred from inelastic scattering experiments performed above the Coulomb barrier. It is hoped that these results may spur this theoretical development as well as provide the stimulus for further experimentation and interpretation particularly for muonic x-ray experiments, inelastic electron-scattering, and inelastic particle-scattering experiments above the Coulomb barrier all of which yield useful information about the intrinsic equilibrium deformation properties of the nucleus.

ACKNOWLEDGMENTS

We would like to thank G. F. Wells and the tandem operating crew for providing the machine development required for these experiments and for providing the copious quantities of ^4He ions consumed during the course of the experiments.

*Research sponsored by the U. S. Atomic Energy Commission under contract with the Union Carbide Corporation.

¹S. G. Nilsson, C. F. Tsang, A. Sobczewski, Z. Szymanski, S. Wycech, C. Gustafson, I. Lamm, P. Moeller, and B. Nilsson, Nucl. Phys. **A131**, 1 (1969); private communication.

²F. A. Gareev, S. P. Ivanova, and V. V. Pashkevitch, Yad. Fiz. **11**, 1200 (1970) [transl.: Sov. J. Nucl. Phys. **11**, 667 (1970)].

³K. Alder, private communication quoting calculations by U. Goetz, H. C. Pauli, and K. Junker; U. Goetz, H. C. Pauli, K. Alder, and K. Junker, Nucl. Phys. **A192**, 1 (1972); H. C. Pauli, Phys. Rep. **7C**, 35 (1973).

⁴V. M. Strutinsky, Nucl. Phys. **A95**, 420 (1967); **A122**, 1 (1968).

⁵D. L. Hendrie, N. K. Glendenning, B. G. Harvey, O. N. Jarvis, H. H. Duhn, J. Sandinos, and J. Mahoney, Phys. Lett. **26B**, 127 (1968).

⁶A. A. Aponick, Jr., C. M. Chesterfield, D. A. Bromley, and N. K. Glendenning, Nucl. Phys. **A159**, 367 (1970).

⁷F. S. Stephens, R. M. Diamond, N. K. Glendenning, and J. de Boer, Phys. Rev. Lett. **24**, 1137 (1970); **27**, 1151 (1971).

⁸T. K. Saylor, J. X. Saladin, I. Y. Lee, and K. Erb, Bull. Am. Phys. Soc. **16**, 1156 (1971); K. A. Erb, J. E. Holden, I. Y. Lee, J. X. Saladin, and T. K. Saylor,

Phys. Rev. Lett. **29**, 1010 (1972); T. K. Saylor, III, J. X. Saladin, I. Y. Lee, and K. A. Erb, Phys. Lett. **42B**, 51 (1972).

⁹A. H. Shaw, J. S. Greenberg, and R. W. Hadsell, Bull. Am. Phys. Soc. **17**, 29 (1972); J. S. Greenberg, private communication.

¹⁰W. Bertozzi, T. Cooper, N. Ensslin, J. Heisenberg, S. Kowalski, M. Mills, W. Turchinets, C. Williamson, S. P. Fivozinsky, J. W. Lightbody, Jr., and S. Penner, Phys. Rev. Lett. **28**, 1711 (1972).

¹¹W. Brückner, J. G. Merdinger, D. Pelte, U. Smilansky, and K. Traxel, Phys. Rev. Lett. **30**, 57 (1973).

¹²P. O. Fröman, K. Dan. Vidensk. Selsk. Mat.-Fys. Skr. **1**, No. 3, (1957).

¹³H. J. Mang and J. O. Rasmussen, K. Dan. Vidensk. Selsk. Mat.-Fys. Skr. **2**, No. 3 (1962); K. Harada, Phys. Lett. **10**, 80 (1964); M. J. Huber, *ibid.* **13**, 242 (1964); J. K. Poggenburg, H. J. Mang, and J. O. Rasmussen, Phys. Rev. **181**, 1967 (1971); S. G. Kadenskii, V. E. Kalechits, and A. A. Martynov, Yad. Fiz. **14**, 343 (1971) [transl.: Sov. J. Nucl. Phys. **14**, 193 (1972)].

¹⁴J. M. Moss, Y. D. Terrien, R. M. Lombard, C. Brassard, J. M. Loiseaux, and F. Resmini, Phys. Rev. Lett. **26**, 1488 (1971).

¹⁵J. L. C. Ford, Jr., P. H. Stelson, C. E. Bemis, Jr., F. K. McGowan, R. L. Robinson, and W. T. Milner, Phys. Rev. Lett. **27**, 1232 (1971); F. K. McGowan,

- C. E. Bemis, Jr., J. L. C. Ford, Jr., W. T. Milner, R. L. Robinson, and P. H. Stelson, *ibid.* 27, 1741 (1971).
- ¹⁶K. Alder, A. Bohr, T. Huus, B. Mottelson, and A. Winther, *Rev. Mod. Phys.* 28, 432 (1956).
- ¹⁷D. L. Hendrie, B. G. Harvey, J. R. Meriwether, J. Mahoney, J.-C. Faivre, and D. G. Kovar, *Phys. Rev. Lett.* 30, 571 (1973).
- ¹⁸C. J. Borkowski and M. K. Kopp, *Rev. Sci. Instrum.* 39, 1515 (1968); *IEEE Trans. Nucl. Sci.* 17, 340 (1970).
- ¹⁹J. L. C. Ford, Jr., P. H. Stelson, and R. L. Robinson, *Nucl. Instrum. Methods* 98, 199 (1972).
- ²⁰L. D. Hunt and C. E. Bemis, Jr., ORNL Chemistry Division Annual Progress Reports Nos. ORNL-4437, 1969 (unpublished), p. 37 and ORNL-4581, 1970 (unpublished), p. 58.
- ²¹B. Grennberg and A. Rytz, *Metrologia* 7, 65 (1971).
- ²²F. K. McGowan, C. E. Bemis, Jr., J. L. C. Ford, Jr., W. T. Milner, P. H. Stelson, and R. L. Robinson, to be published.
- ²³W. T. Milner, unpublished results, 1972.
- ²⁴A. Winther and J. de Boer, in *Coulomb Excitation*, edited by K. Alder and A. Winther (Academic, New York, 1966), p. 303.
- ²⁵K. Alder, F. Roesel, and R. Morf, *Nucl. Phys.* A186, 499 (1972); *Phys. Lett.* 32B, 645 (1970).
- ²⁶G. D. Symons and A. C. Douglas, *Phys. Lett.* 24B, 11 (1967).
- ²⁷M. Schmorak, C. E. Bemis, Jr., M. J. Zender, N. B. Gove, and P. F. Dittner, *Nucl. Phys.* A178, 410 (1972).
- ²⁸F. K. McGowan, W. T. Milner, R. L. Robinson, and P. H. Stelson, *Bull. Am. Phys. Soc.* 16, 493 (1971); W. T. Milner, F. K. McGowan, R. L. Robinson, and P. H. Stelson, *ibid.* 16, 1157 (1971).
- ²⁹O. Nathan and S. G. Nilsson, in *Alpha-, Beta-, and Gamma-Ray Spectroscopy*, edited by K. Siegbahn (North-Holland, Amsterdam, 1965), Vol. 1, p. 640.
- ³⁰N. MacDonald, *Phys. Lett.* 10, 334 (1964).
- ³¹D. Cline, University of Rochester Report No. UR-NSRL-22, July 1969 (unpublished); *Bull. Am. Phys. Soc.* 14, 726 (1969).
- ³²R. P. Scharenberg, J. A. Thompson, W. R. Lutz, R. D. Larsen, and R. G. Kerr, *Bull. Am. Phys. Soc.* 17, 726 (1972).
- ³³A. R. Barnett and W. R. Phillips, *Phys. Rev.* 186, 1205 (1969).
- ³⁴Y. N. Kim, *Mesic Atoms and Nuclear Structure* (North-Holland, Amsterdam, 1971), Chap. 3.
- ³⁵J. R. Nix, private communication.
- ³⁶S. A. DeWitt, G. Backenstoss, C. Daum, J. C. Sens, and H. L. Acker, *Nucl. Phys.* 87, 657 (1967).
- ³⁷E. Eichler, N. R. Johnson, R. O. Sayer, D. C. Hensley, and L. L. Riedinger, *Phys. Rev. Lett.* 30, 568 (1973).
- ³⁸G. R. Satchler, *Phys. Lett.* 39B, 495 (1972).
- ³⁹J. A. Monard, P. G. Huray, and J. O. Thompson, *Bull. Am. Phys. Soc.* 17, 86 (1972); P. G. Huray, J. Monard, and J. O. Thompson, Oak Ridge National Laboratory Report No. ORNL-4743, 1972 (unpublished); J. A. Monard, Oak Ridge National Laboratory Report No. ORNL-TM-3931, August 1972 (unpublished).
- ⁴⁰R. Meeker, G. M. Kalvius, B. D. Dunlap, S. L. Ruby, and D. Cohen, *Bull. Am. Phys. Soc.* 17, 85 (1972).
- ⁴¹H. Ton, W. Beens, S. Roodbergen, and J. Blok, *Nucl. Phys.* A155, 235 (1970).
- ⁴²T. H. Braid, R. R. Chasman, J. R. Erskine, and A. M. Friedman, *Phys. Rev. C* 1, 275 (1970); 4, 247 (1971); *Phys. Rev. C* 4, 1374 (1972).
- ⁴³R. R. Chasman, *Phys. Rev. C* 3, 1803 (1971).